FULL PAPER
THE ANALYST
www.rsc.org/analyst

The air–liquid interface of benzene, toluene, *m*-xylene, and mesitylene: a sum frequency, Raman, and infrared spectroscopic study

Elizabeth L. Hommel and Heather C. Allen*

The Ohio State University, Department of Chemistry, 100 West 18th Ave., Columbus, Ohio 43210, USA. E-mail: allen@chemistry.ohio-state.edu

Received 24th January 2003, Accepted 27th March 2003
First published as an Advance Article on the web 10th April 2003

The air–liquid interface and the liquid-phase of benzene, toluene, 1,3-dimethylbenzene, and 1,3,5-trimethylbenzene are studied using broad bandwidth sum frequency generation spectroscopy, Raman and infrared spectroscopy. A vibrationally resonant sum frequency response is observed from these surfaces in spite of the small hyperpolarizabilities, in particular, the zero and near-zero hyperpolarizabilities of benzene and 1,3,5-trimethylbenzene. The orientation of the aromatic rings of these compounds at their air–liquid interfaces is tilted relative to the surface plane. Thus, on average, the plane of the aromatic ring does not lie in the interfacial plane. Comparison of the square root of the sum frequency intensity to that of the Raman multiplied by the infrared intensity provides additional information about the molecular environment at their respective air–liquid interface.

Introduction

Aromatic hydrocarbons, including benzene, toluene, *m*-xylene, and mesitylene have been measured in significant concentrations in the atmosphere of urban regions,[1,2] and in surface and ground water.[3–5] These compounds are emitted into the environment from many sources,[6] including fuel combustion.[7,8] In the environment, aromatic hydrocarbons may exist in the gas phase, the liquid or particle phase or as an adsorbate on existing particles such as sediments or atmospheric aerosols.[1,2] Many of these hydrocarbons pose health risks in their emitted form and/or can react to form mutagenic compounds.[9–11] Therefore, these studies are a first step in a series of planned interfacial experiments investigating the role that benzene and its derivatives have on surface reaction pathways. Orientation of these molecules at a surface is an important factor when considering surface reaction mechanisms.

The structure of benzene, toluene, *m*-xylene, and mesitylene at various gas–liquid and solid–liquid interfaces are important to understand since they persist in our environment. Yet, the orientation of these molecules at their air–liquid interfaces has not been directly probed previously. This was due to lack of surface-selective experimental techniques with orientation-sensitivity applicable to the study of interfaces at atmospheric pressures. Although there exists several complementary surface sensitive techniques such as UV-photoelectron spectroscopy,[12] neutron reflection spectroscopy,[13] inelastic neutron spectroscopy,[14] X-ray reflection,[15] and X-ray absorption spectroscopy,[16] even-ordered nonlinear spectroscopies (*e.g.* sum and difference frequency) are the only spectroscopic techniques with selection rules that include lack of inversion symmetry. Thus, SFG provides unique information about the air–liquid interface.

In the spectroscopic studies presented here, benzene, toluene, 1,3-dimethylbenzene (*m*-xylene), and 1,3,5-trimethylbenzene (mesitylene) have been selected to systematically study the structure of these molecules at their respective air–liquid interfaces. These studies are the first sum frequency generation (SFG) accounts to be reported from the air–liquid interfaces of benzene, toluene, *m*-xylene and mesitylene. The broad bandwidth sum frequency generation (BBSFG) spectra show that sum frequency symmetry forbidden modes for benzene do in fact arise at its liquid surface. Even though benzene is centrosymmetric with zero hyperpolarizability, β,[17,18] we observe a strong sum frequency response from the air–liquid interface of neat benzene arising from resonant CH vibrational transitions. This is intriguing in that it implies that a dipole is induced in benzene when benzene exists in its air–liquid interfacial region. Equally interesting is the comparison of the toluene, *m*-xylene, and mesitylene surface spectra. Complete cancellation of sum frequency from the methyl symmetric stretching modes due to the symmetry of these vibrations for mesitylene would be expected to occur from a simple vector addition model. Yet, this does not happen.

Sum frequency generation background

SFG is essential to the air–liquid interfacial studies, thus a brief overview is given. A more in depth account of the sum frequency generation theory is found in the literature.[19–26] As a surface-sensitive spectroscopic technique, SFG has been used to study a variety of surfaces and interfaces relevant to surface science and material science.[25,27–33] More recently, SFG has been applied to study solid and liquid surfaces of atmospheric relevance.[24,34–38]

SFG spectroscopy is a second order nonlinear optical technique where the macroscopic nonlinear susceptibility, $\chi^{(2)}$, is probed. The macroscopic polarization of the medium is described in the electric dipole approximation shown in eqn. (1). Where the E represents an electric field and the

$$P = \chi^{(1)}\cdot E + \chi^{(2)}:EE + \chi^{(3)}\vdots EEE + \ldots \quad (1)$$

respective χs represent the polarizability of the medium. The second-order macroscopic nonlinear susceptibility, $\chi^{(2)}$, is probed in SFG experiments. Within the electric dipole approximation, only environments lacking inversion symmetry will give rise to the SFG response. Therefore, at an interface the asymmetry of the interface needs to be taken into account. The SFG intensity, I_{SFG}, is shown in eqn. (2a) where the intensity is

$$I_{SFG} \propto |\chi^{(2)}|^2 I(\omega_{IR}) I(\omega_{800}) \quad (2a)$$

 DOI: 10.1039/b301032p

proportional to the absolute square of the macroscopic nonlinear susceptibility, $\chi^{(2)}$, and the intensity of both the 800 nm, $I(\omega_{800})$, and the infrared, $I(\omega_{IR})$, beams. The nonlinear susceptibility is described in eqn. (2b) where it is broken down into a non-

$$\left|\chi^{(2)}\right| = \left|\chi^{(2)}_{NR} + \sum_{v} \chi^{(2)}_{v}\right| \quad (2b)$$

resonant term, $\chi^{(2)}_{NR}$, and the sum of the resonant terms, $\chi^{(2)}_{v}$. The resonant response dominates the nonlinear susceptibility when the frequency of an incident infrared beam, ω_{IR}, is resonant with a vibrational mode, v, and the intensity of the resultant SFG is enhanced. The resonant macroscopic nonlinear susceptibility, $\chi^{(2)}_{v}$, is shown in eqn. (3), where A_v is the strength of the v^{th}

$$\chi^{(2)}_{v} \propto \frac{A_v}{\omega_v - \omega_{IR} - i\Gamma_v} \quad (3)$$

transition moment and the relative phase between two peaks is denoted by the sign of A_v. The center frequency of the transition moment is represented by ω_v and the dampening factor, Γ_v, describes the half-width at the half-maximum (HWHM) of the transition. The amplitude, A_v, includes both the Raman and the infrared contributions; therefore, the SFG is allowed when the vibrational transition is both Raman and infrared active. To further illustrate this point the molecular susceptibility can be described by eqn. (4), where $<g|\alpha_{lm}|v>$ represents the Raman

$$\beta_{lmn,v} = \frac{\langle g|\alpha_{lm}|v\rangle\langle v|\mu_n|g\rangle}{\omega_{IR} - \omega_v + i\Gamma_v} \quad (4)$$

transition moment and $<v|\mu_n|g>$ represents the IR transition moment of the molecule. An Euler angle transformation relates the molecular coordinate system *(l,m,n)* to the laboratory coordinate system *(I,J,K)*.[22,39,40] The transformation is shown in eqn. (5) where $\mu_{IJK:lmn}$ is the Euler angle transformation

$$\beta_{IJK,v} = \sum_{lmn} \mu_{IJK:lmn}\beta_{lmn,v} \quad (5)$$

between the laboratory-coordinates *(I,J,K)* and the molecule-coordinates *(l,m,n)*.

The macroscopic susceptibility, $\chi_{IJK,v}$, is calculated from the molecular susceptibility, $\beta_{IJK,v}$, as shown in eqn. (6), where

$$\chi^{(2)}_{IJK,v} = N\langle\beta_{IJJ,v}\rangle \quad (6)$$

$\chi_{IJK,v}$ is equal to the number density, N, multiplied by the orientational average of $\beta_{IJK,v}$.

Typically, vibrational SFG experiments are accomplished by combining a narrow bandwidth visible laser pulse with a narrow bandwidth infrared laser pulse. The infrared beam is scanned across the region of interest and the SFG intensity arises when the infrared photons are resonant with an infrared and Raman allowed transition of the molecules at the surface. In the present study, femtosecond broad bandwidth technology is employed. The BBSFG system utilizes a broad bandwidth IR beam ($\sim$600 cm^{-1} bandwidth, $\sim$100 fs pulse duration) rather than a narrow IR bandwidth beam as is used in scanning SFG technologies. Therefore, scanning of the infrared frequency is not necessary. As a result, the vibrational SFG spectrum can be obtained theoretically within one laser pulse leading to shorter acquisition times, larger SFG signals and thus, better signal to noise ratios as compared to scanning SFG spectroscopy instruments. BBSFG spectroscopy was utilized in these experiments.

Experimental

Chemicals

Benzene (99.9+%), toluene (99.8%), *m*-xylene (99+%), and mesitylene (98%) were obtained from Aldrich and used as received. Pyrex petri dishes, used for sample containment for SFG analysis, were cleaned with ammonium persulfate and rinsed with copious amounts of ultrapure water with a resistivity of 18 MΩ cm, then dried in an oven.

Instrumentation

The Raman spectra were obtained using 88 mW from a 532 nm continuous wave laser (Spectra-Physics (SP), Millennia II), a 500 mm monochromator (Acton Research, SpectroPro 500i; 1200 g mm^{-1} grating blazed at 750 nm), and a liquid nitrogen cooled CCD camera (Roper Scientific, LN400EB, 1340 × 400 pixel array, back-illuminated, and deep depletion CCD). Raman spectra were collected using a fiber optic (Inphotonics, RP 532–05–15–FC), which was coupled to the entrance slit of the monochromator. The slit width was set to 10 μm and the resulting spectral resolution was 0.4 cm^{-1}. The Raman spectra were acquired with 1 s exposures to the CCD and 5 spectra were averaged.

The infrared spectra were collected using a Fourier transform infrared spectrometer with a spectral resolution of 4 cm^{-1} (PerkinElmer, 16 PC FT-IR). A drop of each liquid was placed between two NaCl plates and 16 scans were collected and averaged. The spectral absorbances of the IR spectra collected were scaled to the infrared spectra from the NIST Chemistry WebBook (available online).

The laser system used to obtain the broadband sum frequency generation spectra has been previously described.[27,36,41,42] However, a brief overview is presented here. The laser system used for the BBSFG experiments includes two regenerative amplifiers (SP, Spitfires). The amplifiers are seeded with sub 50 fs, 800 nm pulses from a Ti:Sapphire Oscillator (SP, Tsunami). The amplifiers are pumped using a Nd:YLF (SP, Evolution30) laser operating at a kHz repetition rate. One of the amplifiers produces 85 fs, 800 nm broadband pulses ($\sim$300 cm^{-1}). The resulting pulses then pump an optical parametric amplifier (SP, OPA-800C) to produce a broadband infrared beam ($\sim$600 cm^{-1}, kHz). The second amplifier is equipped with a mask that spectrally narrows the pulse to 17 cm^{-1} ($\sim$2 ps). To further narrow the pulse spectrally, an additional mask was added to the compressor within this regenerative amplifier resulting in $\sim$5 cm^{-1} spectral-width pulses.[36] The infrared beam (P-polarized) energy was 11.3 μJ and the visible beam (S-polarized) energy was 150 μJ for this experiment. The infrared and the 800 nm beams were overlapped spatially and temporally on the liquid surface of interest. The resultant sum frequency was dispersed spectrally using a 500 mm monochromator equipped with a 1200 g mm^{-1} diffraction grating blazed at 750 nm (Acton Research, SpectroPro 500i) and the dispersed sum frequency light was collected using a liquid nitrogen cooled CCD camera (Roper Scientific, LN400EB, 1340 × 400 pixel array, back-illuminated CCD). The BBSFG spectra obtained were S-polarized and a Glan laser polarizer was used to verify the resultant BBSFG S-polarization. The spectra were obtained during 5 min acquisitions.

Prior to collecting the BBSFG spectra from the samples, a non-resonant BBSFG spectrum from the surface of a GaAs crystal was obtained during each experimental session. The BBSFG spectra, which are then normalized with the GaAs spectrum, show a central region where the peaks are easily discernable above the noise ($\sim$400 cm^{-1}). As one would expect, the edges of these normalized spectra are dominated by noise; thus, only the central region is used for data presentation and interpretation.

The BBSFG spectra were calibrated using a polystyrene thin film and another non-resonant BBSFG spectrum from the same GaAs crystal. The calibration BBSFG spectrum was collected by placing a thin film of polystyrene (infrared absorbencies are well known) in the path of the infrared beam prior to beam

overlap on the GaAs crystal. The resultant infrared beam is structured due to absorbance by the polystyrene film, which leads to a structured non-resonant BBSFG spectrum from the GaAs crystal. The peak positions (dips) in the calibration GaAs BBSFG spectrum are used to calibrate the BBSFG spectra obtained during the same experimental session.

Results and discussion

The Raman, IR, and SSP-polarized broad-bandwidth sum frequency generation (BBSFG) spectra of benzene, toluene, *m*-xylene, and mesitylene from 2700 cm^{-1} to 3150 cm^{-1} are shown in Fig. 1. Peak assignments were based upon symmetry arguments and assignments from Green[43] and assignments compiled by Varsanyi.[44] Also shown in Fig. 1 are the calculated fits using a Voigt profile[45] with the component peaks for each spectrum. The assignments to the peaks shown in the spectra of Fig. 1, including possible combination and overtone modes, are listed in Table 1. The focus of this paper is on the methyl group stretching modes and the aromatic CH stretching modes. Vertical lines are shown in Fig. 1 passing through the methyl symmetric stretching (CH_3-SS) peaks and the CH stretch region of the Raman, IR, and surface BBSFG spectra for each compound for reference.

The Raman, IR, and surface BBSFG spectra of liquid benzene are shown in the Fig. 1(a1), 1(a2), and 1(a3), respectively. The aromatic CH stretching modes (peaks above 3000 cm^{-1}) observed in these spectra are illustrated in Fig. 2 and correspond to benzene vibrational modes from Varsanyi.[44] To be able to compare relative intensities within each spectroscopic technique, the scale for each type of spectrum is kept constant. Since the benzene signal is off scale, the full scale benzene spectrum is shown as an inset to Fig. 1(a1). In some cases, different aromatic CH modes are observed in each type of spectroscopy as one would expect from symmetry of the vibrational modes. In the surface BBSFG spectrum from benzene, the peak observed at 3056 cm^{-1} is assigned to the degenerate ν_{20a} and ν_{20b} CH vibrational modes, which are shown in Fig. 2.

The significant surface BBSFG response from the neat benzene–air interface as shown in Fig. 1(a3) was not an anticipated result since benzene is centrosymmetric and the first hyperpolarizability, β, of benzene is zero.[17,18] The benzene molecules at the surface experience a different environment on the air-side *versus* the liquid-side of the interface. Therefore, distortions in the electron density of the benzene may explain the observation of a peak due to a symmetry forbidden mode in our BBSFG spectrum.

The P-polarized IR used in this experiment efficiently probes only the transition moments that have components perpendicular to the surface plane. Thus, detection of the CH modes requires that the benzene molecules are on average perpendicular to the surface plane. An entropically favored surface drives the molecules to stack against one another with benzene rings perpendicular to the surface plane. EFISH (electric field induced second harmonic generation) measurements of neat benzene show that upon application of a DC field to the liquid, a second harmonic signal is detected, probing the second

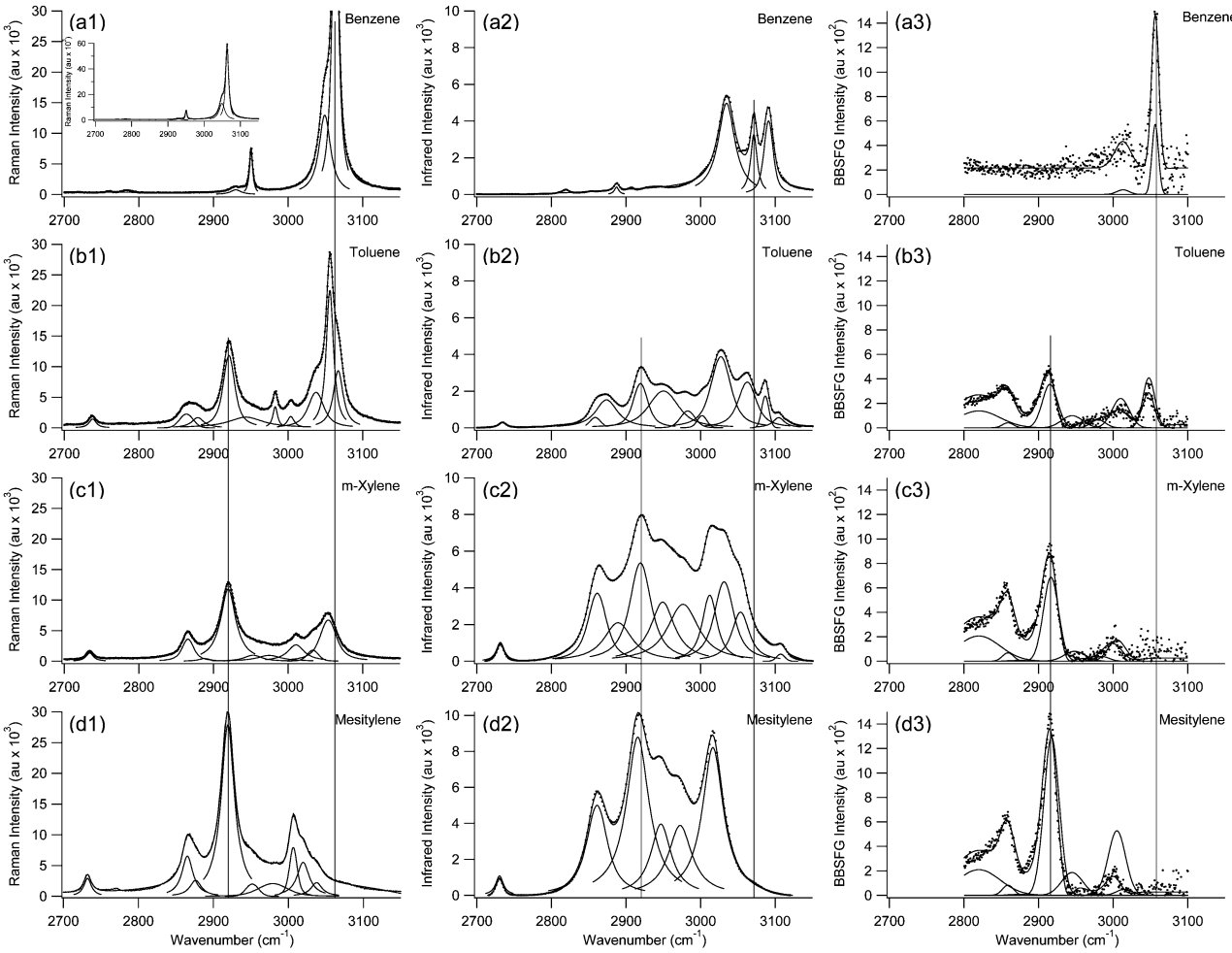

Fig. 1 Raman (column 1), IR (column 2), surface BBSFG (column 3) spectra of benzene (row a), toluene (row b), *m*-xylene (row c), and mesitylene (row d). The individual deconvoluted peaks are also shown. Vertical lines are drawn to aid the eye for relative peak positions.

hyperpolarizability, γ.[17] However, in our experiments an electric field is not applied, yet the induced dipole established in the interfacial region combined with asymmetry with respect to the inversion center in the ν_{20a} and ν_{20b} vibrational modes gives rise to the SFG response.

The CH stretching mode frequencies in the BBSFG spectrum from benzene (Fig. 1(a3)) shift to lower frequencies as compared to the IR spectra (Fig. 1(a2)). Since sum frequency is probing the air–liquid benzene interface, a change in frequencies is not surprising.

The Raman, IR, and surface BBSFG spectra of liquid toluene are shown in Fig. 1(b1), 1(b2), and 1(b3), respectively. The peaks observed at 2921 cm^{-1}, 2919 cm^{-1}, and 2915 cm^{-1} in the Raman, IR and surface BBSFG spectra of toluene, are assigned to the methyl symmetric stretch (CH_3-SS) mode, respectively. The peaks observed at 2944 cm^{-1} and 2983 cm^{-1} in the toluene Raman spectrum, 2950 cm^{-1} and 2983 cm^{-1} in the toluene IR spectrum, and 2945 cm^{-1} and 2980 cm^{-1} in the toluene BBSFG spectrum are attributed to the methyl asymmetric stretching (CH_3-AS) modes. The CH stretching modes, listed in Table 1 for toluene, show that the surface BBSFG is only observed from the ν_{20a} and ν_2 vibrations for the CH stretching modes of the aromatic ring. However, a significant frequency shift is observed from the BBSFG benzene CH assignments, as one would expect. In addition, the aromatic CH stretching mode frequencies in the BBSFG spectrum from toluene shift to lower frequencies as compared to the Raman and IR spectra. The sign of the amplitude of the individual component peaks calculated using a Voigt profile[45] of the toluene BBSFG spectrum determined that the CH_3-AS transitions were 90° out of phase with the CH_3-SS, and all of the aromatic CH transitions were in phase with the CH_3-AS.

The Raman, IR, and surface BBSFG spectra of liquid *m*-xylene (1,3-dimethylbenzene) are shown in Fig. 1(c1), 1(c2), and 1(c3), respectively. The peaks observed at 2920 cm^{-1}, 2919 cm^{-1}, and 2917 cm^{-1} in the Raman, IR, and BBSFG spectra of *m*-xylene, respectively, are attributed to the CH_3-SS. Additionally, the peaks observed at 2953 cm^{-1} and 2975 cm^{-1} in the Raman spectrum, 2949 cm^{-1} and 2976 cm^{-1} in the IR spectrum, and 2948 cm^{-1} and 2985 cm^{-1} in the BBSFG spectrum are assigned to the CH_3-AS modes. The aromatic CH stretching modes, listed in Table 1 for *m*-xylene, show that the surface BBSFG is observed from the ν_2 and ν_{20b} aromatic ring vibrational structure shown in Fig. 2, and that for Raman, IR, and the surface BBSFG, the ν_{7a} mode is no longer relevant and the ν_{7b} structure is below the experimental range.[44] The ν_2 and ν_{20b} assignments are based on symmetry of the vibrational mode and assignments from Green.[43] However, we have not completely ruled out the ν_{20a} assignment for this peak. The sign of the amplitude of the individual component peaks calculated using a Voigt profile[45] of the *m*-xylene BBSFG spectrum determined that the CH_3-AS transitions were 90° out of phase with the CH_3-SS and all of the aromatic CH transitions were in phase with the CH_3-AS.

The Raman, IR, and surface BBSFG spectra of liquid mesitylene (1,3,5-trimethylbenzene) are shown in Fig. 1(d1), 1(d2), and 1(d3), respectively. The peaks observed at 2919 cm^{-1}, 2916 cm^{-1}, and 2917 cm^{-1} in the mesitylene Raman, IR, and BBSFG spectra, respectively, are assigned to the CH_3-SS. The peaks observed at 2952 cm^{-1} and 2979 cm^{-1} in the Raman spectrum, 2947 cm^{-1} and 2972 cm^{-1} in the IR spectrum, and 2946 cm^{-1} and 2973 cm^{-1} (barely visible in Fig. 1(d3)) in the surface BBSFG spectrum are attributed to the CH_3-AS modes. The CH stretching modes, listed in Table 1 for mesitylene, show that the surface BBSFG is observed from the ν_{20a} and ν_{20b} aromatic ring vibrational structure shown in Fig. 2. For the Raman, IR, and the BBSFG, the ν_{7a} and ν_{7b} modes are below the experimental range.[44] The sign of the amplitude of the individual component peaks calculated using a Voigt profile[45] of the mesitylene BBSFG spectrum determined that the two CH_3-AS transitions were 90° out of phase with the CH_3-SS and all of the aromatic CH transitions were in phase with the CH_3-AS.

The Raman and IR spectra of toluene, *m*-xylene, and mesitylene are expected to have peaks in the spectral region above 3000 cm^{-1} due to the aromatic CH stretching modes. The peaks observed below 3000 cm^{-1} are mainly assigned to methyl group vibrational modes as discussed above. Although the aromatic CH spectral region for toluene, shown in Fig. 1(b1) and 1(b2) resemble that of benzene, the aromatic CH spectral

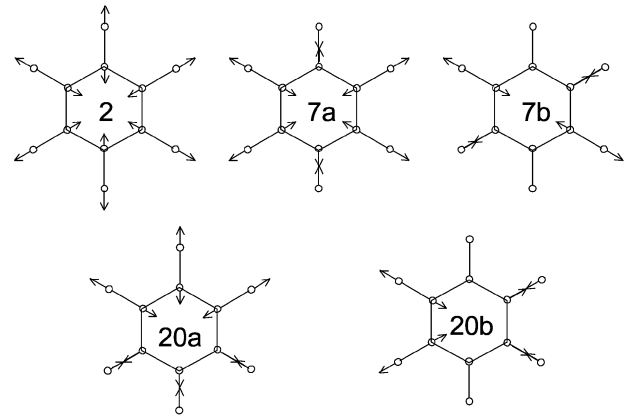

Fig. 2 The benzene vibrational modes adapted from Varsanyi.[44]

Table 1 Summary of the peak assignments

	Benzene (D_{6h})				Toluene (C_{2v})				*m*-Xylene (C_{2v})				Mesitylene (D_{3h})			
	Raman	IR	BBSFG	Lit	Raman	IR	BBSFG	Lit	Raman	IR	BBSFG	Lit	Raman	IR	BBSFG	Lit
Comb/overtone	—	—	—	—	2738	2734			2734	2732			2732	2730		
Comb/overtone	—	—	—	—	2864	2859	2859		2866	2861	2859		2865	2861	2859	
Comb/overtone	—	—	—	—	2879	2874			2888	2889	2875		2876		2875	
ν_s (CH_3)	—	—	—	—	2921	2919	2915	2921[a]	2920	2919	2917	2923[a]	2919	2916	2917	2917[a]
ν_a (CH_3)	—	—	—	—	2944	2950	2945	2952[a]	2953	2949	2948	2953[a]	2952	2947	2945	2946[a]
ν_a (CH_3)	—	—	—	—	2983	2983	2980	2979[a]	2975	2976	2985	2970[a]	2979	2972	2975	2973[a]
Comb/overtone	2950	2887							3011	3012	3005		3007		3005	
ν (=CH) 7a	3049	—		3056[a]	3004	3002	3010	3003[a]				—				935[a]
ν (=CH) 7b	3049	—		3056[a]	3037			3039[a]				903[a]				935[a]
ν (=CH) 20a	—	3071	3056	3064[a]	3067	3063	3048	3063[a]	3033	3031		3032[b]	3020	3016	3015	3017[a]
ν (=CH) 20b	—	3071	3056	3064[a]		3027		3029[a]	3054	3054	3045	3052[b]	3020	3016	3015	3017[a]
ν (=CH) 2	3063			3073[a]	3056			3055[a]	3054	3054	3045	3052[b]				3020[a]
Comb/overtone		3034	3013			3087							3038			
Comb/overtone		3091				3105				3107						

[a] Varsanyi.[44] [b] Green.[43]

region has shifted slightly to lower frequencies. The aromatic CH stretches for *m*-xylene and the mesitylene are further shifted to lower frequencies in the Raman and IR spectra; the highest frequency for an aromatic CH stretch in the mesitylene spectra is 40 cm^{-1} less than the lowest frequency aromatic CH stretch observed from benzene. An intramolecular interaction of an eclipsing methyl group or intermolecular interactions of non-eclipsing methyl groups with adjacent aromatic rings may be causing the observed red shifts. A previous computational investigation of benzene and several substituted benzenes led to the determination that the preferred orientation of the methyl group has one CH bond eclipsing the benzene ring of toluene, m-xylene and mesitylene in the gas phase.[46] The interaction of the eclipsing methyl hydrogen with the aromatic ring will result in a red shift for the aromatic CH stretching modes. The red shift in the peaks assigned to the aromatic –CH stretching modes infers that the methyl groups contained on the benzene rings prefer the eclipsing conformer. The interpretation of the preferred eclipsing conformer is also consistent with a Raman and IR study of crystalline toluene, although inconsistent with the interpretation from their liquid studies.[47] X-ray diffraction studies of xylene crystals do not support the eclispsing conformer model.[48,49] The BBSFG spectra are expected to have characteristics from both the Raman and the IR spectra, since the transition moment is a combination of the Raman transition and the IR transition moments. However, the BBSFG spectrum of mesitylene is expected to have small intensities, since β is nearly zero.[18] Nonetheless, the surface BBSFG spectrum of mesitylene is well resolved with a relatively large SFG response. The surface BBSFG spectrum of mesitylene detected at the air–liquid interface is due to an interfacial induced dipole, similar to the interfacial effects on benzene. The resulting surface BBSFG spectra of toluene, *m*-xylene and mesitylene do contain spectral characteristics analogous to their respective Raman and IR spectra.

The observed positions for the peaks assigned to the CH_3-SS in the Raman, IR, and BBSFG spectra for toluene, *m*-xylene, and mesitylene all occur within 6 cm^{-1} of each other; the vertical line drawn in Fig. 1 through the CH_3-SS peaks further illustrates the minimal differences in the spectra. However, significant differences are observed in the methyl peak integrated areas for the spectra shown in Fig. 1. To further illustrate how the methyl peak areas vary as a function of the number of methyl group moieties, the Raman, IR, and BBSFG methyl peak areas are plotted in Fig. 3. The relative areas for the Raman, IR, and BBSFG spectral peaks assigned to the CH_3-SS (diamonds) and the individual peaks assigned to the two CH_3-AS (squares and triangles) *versus* the number of methyl groups contained in the molecule are shown in Fig. 3, where (a) is the Raman data, (b) is the IR data, and (c) is the square root of the BBSFG data. The relative peak areas of the CH_3-SS in the toluene (1 CH_3 moiety) spectra have the lowest integrated peak area for all three of the spectroscopic techniques utilized. The integrated peak areas for the CH_3-SS in the *m*-xylene (2 CH_3) spectra are larger than that of toluene, yet the CH_3-SS in the mesitylene (3 CH_3) spectra have the largest integrated peak areas. This result is not surprising since the response from all three spectroscopic techniques is proportional to the number density of the moieties being evaluated. However, the peak areas of the CH_3-AS do not scale with the increasing number of methyl groups as one might expect, in particular the Raman and BBSFG spectra of toluene, *m*-xylene, and mesitylene do not follow any apparent trends. The transition moment of the Raman asymmetric stretching mode is relatively weak; therefore, any changes in the peak intensity are difficult to differentiate.

The surface SFG response for a vibrational mode is proportional to the Raman transition moment multiplied by the IR transition moment and convoluted with molecular orientation at the surface. In Fig. 4, the square root of the CH_3-SS Raman peak area multiplied by the square root of the corresponding IR peak area is plotted. The square roots of the CH_3-SS peak areas of the BBSFG peaks are also shown in Fig. 4. The slope of the line through the peak areas for the surface BBSFG CH_3-SS (solid diamonds) is substantially smaller than the slope of the line through the Raman CH_3-SS multiplied by the IR CH_3-SS (hollow diamonds) as observed in Fig. 4. The smaller slope due to the BBSFG CH_3-SS is attributed to surface orientation and intramolecular cancellation of the stretching modes.

The SFG response from the CH_3-SS for all three of the methyl-substituted benzenes strongly indicates that the molecules are aligned with the benzene rings on average tilted from the surface plane. The transition moment for the CH_3-SS is aligned along the central axis of the methyl group and is contained within the plane of the benzene ring. Therefore, the ring must be tilted from the surface plane for interactions between the P-polarized IR and the CH_3-SS to occur. Furthermore, the peak position of the CH_3 stretching modes observed in the surface BBSFG spectra are nearly the same frequency or red-shifted as compared to the liquid IR and Raman stretching frequencies of the same transition as shown in

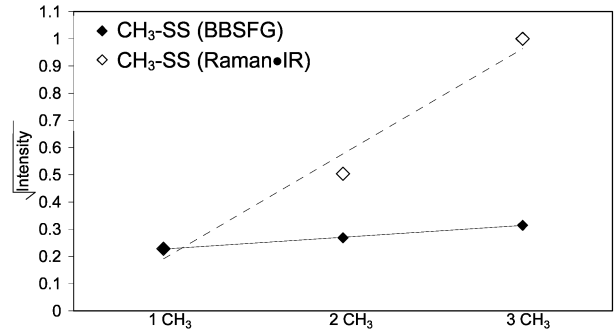

Fig. 4 The square root of the BBSFG intensity (solid diamonds) and the square root of the Raman intensity times the square root of the IR intensity (hollow diamonds). The BBSFG intensities are normalized to the Raman·IR intensities using the toluene CH_3-SS intensity.

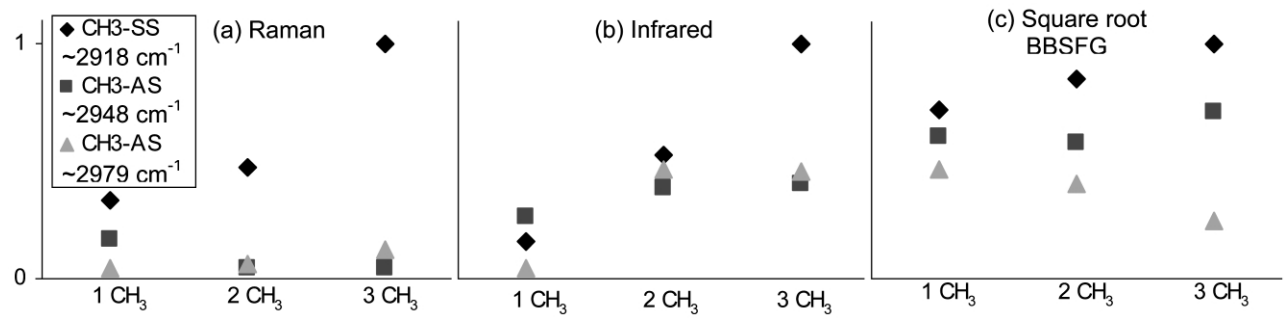

Fig. 3 The integrated peak areas for the CH_3-SS (◆ 2918 ± 2 cm^{-1}) and CH_3-AS (■ 2948 ± 3 cm^{-1} and ▲ 2979 ± 4 cm^{-1}) for toluene (1 CH_3), *m*-xylene (2 CH_3), and mesitylene (3 CH_3); (a) is the Raman intensity, (b) is the IR intensity, and (c) is the square root of the surface BBSFG intensity.

Table 1. Previous measurements have shown that the gas phase peaks are blue shifted as compared to the liquid phase frequencies for these compounds.[50] Considering the surface BBSFG peak positions one could conclude that the methyl groups experience a more liquid-like environment; therefore, in the toluene and *m*-xylene interfacial regions the methyl groups are oriented on average toward the liquid. The mesitylene however cannot orient all of its methyl groups on the same side of the interface. Yet, on average two of the mesitylene methyl groups may exist on the liquid side.

The symmetry of mesitylene implies that the sum frequency response from the CH_3-SS transition moments may cancel each other out. However, at the interface the transitions due to the CH_3-SS exposed to the air environment arise at a different frequency as compared to the transitions due to the CH_3-SS exposed to the liquid environment. The different frequencies infer a change in the character of the transition of each stretching mode; therefore, the SFG response from the liquid-side CH_3-SS mode cannot efficiently cancel the SFG response from the air-side CH_3-SS mode.

Conclusions

In summary, we have studied a select group of methyl-substituted benzenes: benzene, toluene, *m*-xylene, and mesitylene. The Raman and IR results are consistent with previously published accounts of these compounds in the investigated region of 2700 cm^{-1} to 3150 cm^{-1}. The predicted SFG response is zero and near-zero for benzene and mesitylene molecules, yet we observe large SFG intensities in their respective surface BBSFG spectra. This result indicates that the interfacial region is capable of producing an induced dipole in polarizable systems, such as benzene. The detection of both the aromatic CH stretching modes and the CH_3-SS modes determines that the molecules must on average be tilted relative to the surface plane. The detected frequencies for the CH_3-SS are liquid-like thus indicating that the methyl portions of the molecules favor the liquid-side of the interface. Furthermore, the lack of cancellation of the CH_3-SS from mesitylene suggests that the effect of air on the stretching mode differs from that of the liquid.

Acknowledgement

This research was funded by the National Science Foundation through The Ohio State University Environmental Molecular Science Institute (NSF Grant No. CHE-0089147). We also thank Professors S. Singer, C. Hadad, and T. Miller for providing helpful comments and discussions.

References

1 M. P. Fraser, G. R. Cass and B. R. T. Simoneit, *Environ. Sci. Technol.*, 1998, **32**, 2051.
2 M. P. Fraser, G. R. Cass, B. R. T. Simoneit and R. A. Rasmussen, *Environ. Sci. Technol.*, 1998, **32**, 1760.
3 B. A. Bekins, I. M. Cozzarelli, E. M. Godsy, H. I. Essaid and M. E. Tuccillo, *J. Contam. Hydrol.*, 2001, **53**, 387.
4 I. M. Cozzarelli, B. A. Bekins, M. J. Baedecker, G. R. Aiken, R. P. Eganhouse and M. E. Tuccillo, *J. Contam. Hydrol.*, 2001, **53**, 369.
5 C. Marianna, *Fresenius Environ. Bull.*, 2002, **11**, 91.
6 Y. M. Kim, S. Harrad and R. M. Harrison, *Environ. Sci. Technol.*, 2001, **35**, 997.
7 W. O. Siegl, R. H. Hammerle, H. M. Herrmann, B. W. Wenclawiak and B. Luers-Jongan, *Atmos. Environ.*, 1999, **33**, 797.
8 J. J. Schauer, M. J. Kleeman, G. R. Cass and B. R. T. Simoneit, *Environ. Sci. Technol.*, 2002, **36**, 1169.
9 Y. Ueno, T. Horiuchi and O. Niwa, *Anal. Chem.*, 2002, **74**, 1712.
10 B. J. Finlayson-Pitts and J. N. Pitts, Jr, *Chemistry of the Upper and Lower Atmosphere: Theory, Experiments and Applications*, Academic Press, San Diego, CA, 2000, ch. 10, pp. 436.
11 S. C. Basak, G. D. Grunwald, B. D. Gute, Balasubrumanian and D. Opitz, *J. Chem. Inf. Comput. Sci.*, 2000, **40**, 885.
12 M. G. Garnier, R. Wahrenberg and P. Oelhafen, *Phys. Rev. B.*, 2002, **65**, 113204.
13 J. R. Lu, Z. X. Li, R. K. Thomas, B. P. Binks, D. Chrichton, P. D. I. Fletcher, J. R. McNab and J. Penfold, *J. Phys. Chem. B*, 1998, **102**, 5785.
14 J. Z. Larese, D. Martin Y Marero, D. S. Sivia and C. J. Carlile, *Phys. Rev. Lett.*, 2001, **87**, 206102.
15 G. E. Brown, Jr, V. E. Henrich, W. H. Casey, D. L. Clark, C. Eggleston, A. Felmy, D. W. Goodman, M. Graetzel, G. Maciel, M. I. McCarthy, K. H. Nealson, D. A. Sverjensky, M. F. Toney and J. M. Zachara, *Chem. Rev.*, 1999, **99**, 77.
16 K. F. Hayes and L. E. Katz, in *Physics and Chemistry of Mineral Surfaces*, ed. P. V. Brady, CRC, Boca Raton, FL, 1996, pp. 147.
17 L.-T. Cheng, W. Tam, S. H. Stevenson, G. R. Meredith, G. Rikken and S. R. Marder, *J. Phys. Chem.*, 1991, **95**, 10631.
18 M. G. Papadopoulos and J. Waite, *J. Chem. Soc., Perkin Trans. II*, 1988, 2055.
19 Y. R. Shen, *The Principles of Nonlinear Optics*, John Wiley & Sons, New York, 1st edn., 1984.
20 C. D. Bain, *J. Chem. Soc., Faraday Trans.*, 1995, **91**, 1281.
21 B. Dick, A. Gierulski and G. Marowsky, *Appl. Phys. B*, 1985, **38**, 107.
22 C. Hirose, N. Akamatsu and K. Domen, *Appl. Spectrosc.*, 1992, **46**, 1051.
23 A. Morita and J. T. Hynes, *Chem. Phys.*, 2000, **258**, 371.
24 M. J. Shultz, S. Baldelli, C. Schnitzer and D. Simonelli, *J. Phys. Chem. B*, 2002, **106**, 5313.
25 A. G. Lambert, D. J. Neivandt, A. M. Briggs, E. W. Usadi and P. B. Davies, *J. Phys. Chem. B*, 2002, **106**, 5461.
26 G. L. Richmond, *Chem. Rev.*, 2002, **102**, 2693.
27 G. Ma and H. C. Allen, *J. Am. Chem. Soc.*, 2002, **124**, 9374.
28 L. J. Richter, T. P. Petralli-Mallow and J. C. Stephenson, *Opt. Lett.*, 1998, **23**, 1594.
29 P. B. Miranda and Y. R. Shen, *J. Phys. Chem. B*, 1999, **103**, 3292.
30 K. A. Briggman, J. C. Stephenson, W. E. Wallace and L. J. Richter, *J. Phys. Chem. B*, 2001, **105**, 2785.
31 C. S.-C. Yang, L. J. Richter, J. C. Stephenson and K. A. Briggman, *Langmuir*, 2002, **18**, 7549.
32 G. Kim, M. Gurau, J. Kim and P. S. Cremer, *Langmuir*, 2002, **18**, 2807.
33 J. Kim, G. Kim and P. S. Cremer, *J. Am. Chem. Soc.*, 2002, **124**, 8751.
34 H. C. Allen, E. A. Raymond and G. L. Richmond, *Curr. Opin. Colloid Interface Sci.*, 2000, **5**, 74.
35 H. C. Allen, E. A. Raymond and G. L. Richmond, *J. Phys. Chem.*, 2001, **105**, 1649.
36 G. Ma and H. C. Allen, *J. Phys. Chem. B*, submitted.
37 D. Simonelli, S. Baldelli and M. J. Shultz, *Chem. Phys. Lett.*, 1998, **298**, 400.
38 C. Raduge, V. Pflumio and Y. R. Shen, *Chem. Phys. Lett.*, 1997, **274**, 140.
39 C. Hirose, N. Akamatsu and K. Domen, *J. Chem. Phys.*, 1992, **96**, 997.
40 C. Hirose, H. Yamamoto, N. Akamatsu and K. Domen, *J. Phys. Chem.*, 1993, **97**, 10064.
41 E. L. Hommel, G. Ma and H. C. Allen, *Anal. Sci.*, 2001, **17**, 1325.
42 E. L. Hommel and H. C. Allen, *J. Phys. Chem. B*, submitted.
43 J. H. S. Green, *Spectrochim. Acta, Part A*, 1970, **26**, 1523.
44 G. Varsanyi, *Assignments for Vibrational Spectra of Seven Hundred Benzene Derivatives*, John Wiley & Sons, New York, 1974, **vol. 1**.
45 All of the spectra were fit using a Voigt profile in Igor 4.05A. The Raman and IR spectra were deconvoluted using the Voigt fit routine included in Igor Pro 4.05A package. The Voigt profile for the BBSFG spectra was written as a separate routine in Igor to account for the coherent nature of the SFG.
46 C. M. Hadad, J. Damewood, R. James and J. F. Liebman, *Tetrahedron*, 1989, **45**, 1623.
47 J. L. Breuil, D. Cavagnat, J. C. Cornut, M. T. Forel, M. Fousassier and J. Lascombe, *J. Mol. Struct.*, 1979, **57**, 35.
48 R. M. Ibberson, W. I. F. David, S. Parsons, M. Prager and K. Shankland, *J. Mol. Struct.*, 2000, **524**, 121.
49 H. van Koningsveld and A. J. van den Berg, *Acta Crystallogr.*, 1986, **B42**, 491.
50 N. Fuson, C. Garrigou-Lagrange and M. L. Josien, *Spectrochim. Acta, Part A*, 1960, **16**, 106.